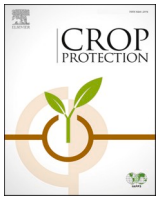
Crop Protection 181 (2024) 106701



Contents lists available at ScienceDirect

Crop Protection

journal homepage: www.elsevier.com/locate/cropro





Innovating an electrostatic charging unit with an insulated induction electrode for air-assisted orchard sprayers

Kemal Amaya *, Ali Bayat

Çukurova University, Faculty of Agriculture, Department of Agricultural Machinery and Technologies Engineering, Adana, Türkiye

ARTICLE INFO

Keywords:
Droplet charging efficiency
Electrostatic spraying
Induction charging method
Air-assisted orchard sprayers

ABSTRACT

Orchard pesticide applications using electrostatic spraying technology enhance droplet deposition and reduce environmental pollution. However, the incorporation of charging systems into conventional air-assisted sprayers remains limited. This is primarily due to challenges such as the necessity for high air velocity to prevent droplet adherence to electrodes, electrode-nozzle design flaws, and safety concerns related to the high voltage used for charging. To address these issues, this study developed five charging units that employ insulated induction electrodes, eliminating exposure to external elements. These units were incorporated into an air-assisted sprayer to assess their effectiveness in charging spray droplets and improving deposition. The units successfully limited electrical leakage, even under high-voltage conditions (up to 18 kV) and in the absence of airflow. At an electrode voltage of 14 kV, and an air velocity of 27 m s^{-1}, the electrostatic units achieved an average charge-to-mass ratio of up to 0.67 mC kg^{-1}. Activation of the charging units significantly enhanced droplet deposition with an increase of 90% on the front and 3250% on the back surfaces of the artificial targets (aluminum plates). On real plant leaves, the increase was 54% on the front and 112% on the back surfaces compared with uncharged standard spraying.

1. Introduction

The application of pesticides to orchard trees is a critical aspect in agricultural management. It plays a vital role in controlling pests, diseases, and weeds, ensuring the healthy growth of crops, and optimizing fruit yield. The effectiveness of pesticide application depends on several factors, including the timing, dosage, and use of environmentally sustainable methods. These considerations are essential to mitigate potential risks to human health and the environment. One of the challenges in achieving successful pesticide application is ensuring that the spray effectively reaches the target surfaces.

Pesticide applications in orchards and vineyards typically use conventional air-assisted sprayers (Göhlich et al., 1996). However, these sprayers have been found to deposit only 46% of spray droplets on tree leaves, with the remainder dispersing to neighboring trees (4%) and adjacent areas (50%) (Garcera et al., 2017). Electrostatic spraying technology can improve deposition due to the attractive forces between charged droplets and plant leaves. The induction charging method is often employed in electrostatic spraying systems developed for pesticide applications (Martin et al., 2022; Pelegrini et al., 2022; Salcedo et al., 2020).

MaxCharge nozzle, developed by Electrostatic Spraying Systems Co. (ESS) using an embedded induction electrode, represents a significant advancement in electrostatic spraying technology. Its design was influenced by foundational research on electrostatic charging and spray dynamics (Frost and Law, 1981; Herzog et al., 1983; Law, 1978; Patel et al., 2016, 2017). These studies provide insights to the mechanisms of droplet charging and the effects of electrostatic forces on spray patterns, which are crucial for the development of an effective and safe electrostatic nozzle. The ability of MaxCharge nozzle to enhance spray deposition on plant targets has been confirmed in recent studies, demonstrating its potential to improve pesticide application efficiency and reduce off-target drift (Pascuzzi and Cerruto, 2015; Salcedo et al., 2020).

Despite the advantages of electrostatic spraying, the high cost of commercial electrostatic sprayers and their suitability for only low-volume applications have limited their adoption for larger trees. To address this issue, researchers have explored retrofitting conventional air-assisted orchard sprayers using induction electrodes of various designs. However, the hazards of high voltage with uninsulated electrodes

* Corresponding author.
E-mail addresses: kemal.amaya86@gmail.com (K. Amaya), alibayat@cu.edu.tr (A. Bayat).

https://doi.org/10.1016/j.cropro.2024.106701
Received 18 July 2023; Received in revised form 5 April 2024; Accepted 11 April 2024
Available online 16 April 2024
0261-2194/© 2024 Elsevier Ltd. All rights reserved.

and electrode wetting causing electrical leakage, are serious issues with this type of electrostatic spraying operation. These issues restrict the application of high voltage levels to the induction electrodes to enhance the charging efficiency and thus increase droplet deposition.

Regardless of the high voltage risks, air-assisted orchard sprayers, which are adapted to utilize electrostatic charging technology, usually use high airflow velocities to prevent electrode wetting and accompanying electrical leakage. Bayat et al. (1994) used an air velocity of 78 m s^{-1} to eliminate electrode wetting when a high voltage of 17 kV was applied to charge droplets produced by an air-assisted orchard sprayer. Similarly, Gan-Mor et al. (2014) had to increase the air-assisted velocity of the sprayer fan until 60 m s^{-1} to overcome the problem at an electrode voltage of 20 kV. Excessively high air velocities can cause charged droplets to drift away from intended plant targets, especially in electrostatic applications for small trees (Miranda-Fuentes et al., 2015; Musiu et al., 2019; Pascuzzi et al., 2017). Furthermore, high air velocities contribute to greater vibrations in spraying equipment, resulting in cumulative damage over time and additional costs.

In an earlier paper, Amaya and Bayat (2023) observed that covering the induction electrode with an insulating layer improves the charge-to-mass ratio of spray droplets by preventing electric leakage, which limits the use of higher voltages. Furthermore, the insulated electrodes completely isolate the electrostatic spraying system from the moist external environment, thereby removing high-voltage hazards to sprayer operators. Therefore, this study aims to (1) develop electrostatic charging units with insulated induction electrodes, which can be mounted on air-assisted conventional orchard sprayers without changing the machine design, and (2) install these charging units onto an air-assisted conventional orchard sprayer to assess their effectiveness in charging spray droplets and increasing deposition on both artificial and plant targets at low air-assisted velocities.

2. Materials and methods

2.1. Manufacturing electrostatic charging units with insulated electrodes

A commercial nozzle, which has a valve-type body (Plastic Turbo Atomizer Nozzle 3/8 E" - Code, 18,020, Başak Pülverizatör Co., Manisa, Türkiye) and two outlets for spraying operations, was used in this study (Fig. 1-A). The first outlet (I) is a full-cone-type nozzle with an adjustable turbulence chamber volume. The other outlet (II) is a standard hollow cone nozzle that provides a constant liquid flow rate for each spraying pressure. The second outlet (II) was mainly used for charging droplets and deposition trials in this study. It consisted of a strainer (1), swirl plate (2), plastic gasket (3), ceramic plate (4) with a 0.8 mm orifice, and head cap (5).

Primary laboratory tests were conducted on outlet (II) of the used nozzle in an effort to enhance the charge-to-mass ratio evaluated with the Faraday cage described in a previous study (Amaya and Bayat, 2023). The findings demonstrated that the charge-to-mass ratios provided by the Brass ConeJet (Brass ConeJet TX6, Spraying Systems Co., Chicago, USA) were more significant than those of the ceramic plate (4) at approximately the same spraying pressures and liquid flow rates. Moreover, using the outward extended ConeJet tip (6 in Fig. 1-B) widens the gap between the nozzle head (5) and the electrode, allowing more air to pass through this gap and more effectively preventing electrode wetting. Therefore, Brass ConeJet TX6 tip was used instead of the ceramic plate in all subsequent charging and deposition experiments.

To produce the insulated induction electrodes (IIE) as shown in Fig. 2 for the electrostatic charging units, a copper rod with a diameter of 6 mm was inserted into a flexible transparent silicone tube, which was used as the dielectric material. The covered rod (1) was used to shape the insulated charging electrodes with inner and outer diameters of 36 and 56 mm, respectively, and a 2-mm silicone insulation layer (2). The high voltage was supplied to the copper electrode within the insulation layer via a high-voltage cable (4) through the connection point (3). The junction region between the high-voltage cable and the electrode insulating layer was closed with a dielectric silicone adhesive (5).

The stability of the insulating substance (2) and the closing region (5) of the high-voltage electrode (1) in Fig. 3 was tested to prevent electric leakage between its surface and adjacent objects, such as liquid spray, under extreme wet circumstances similar to those found in pesticide applications. Each insulated electrode was immersed in grounded water in a plastic pot (6). Subsequently, it was exposed to a high voltage of 18 kV for approximately 15 min using a high-voltage source (7) (Model Vsm 2016, Udescon Co., Istanbul, Türkiye). Throughout this period, a digital voltmeter device (8) (Model Ut33d, Uni-Trend Technology Co., Dongguan, China) continually measures the applied high voltage, through a high-voltage probe (9) (Model Pd-28, Standard Electric Works Co., New Taipei, Taiwan). The sudden decline in the measured high-voltage value to zero indicates electrical leakage between the electrode and the earthing wire across the water. This indicates an issue with the electrical insulation of the tested electrode, which should be repaired before installation on the nozzle.

To produce each electrostatic charging unit, one insulated electrode, tested at 18 kV for 15 min, was fixed in front of the orifice of each nozzle, as shown in Fig. 4. The distance between the nozzle orifice and the electrode, adjustable by the connection tools (5), was selected so that it provides the most significant charge-to-mass ratio. Five insulated induction electrodes with identical specifications were produced and mounted on the right side of the turbulence chamber of an air-assisted orchard sprayer (Lotus F20, Önallar Co., Konya, Türkiye) to assess the charge-to-mass ratio and droplet deposition.

2.2. Evaluation of the charge-to-mass ratio of the charging units on the sprayer

Fig. 5 shows the method of measuring the electric current of the charged droplets produced by the electrostatic units mounted on the

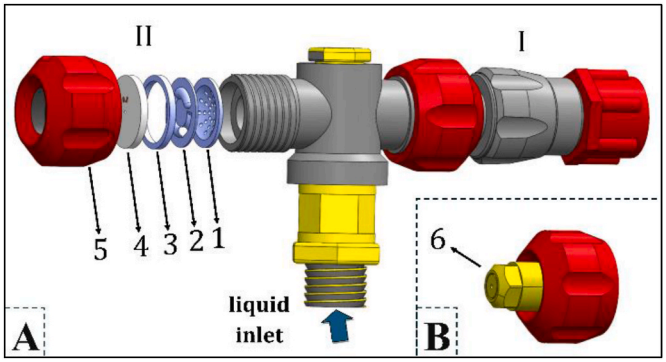


Fig. 1. Hydraulic nozzle used to develop the electrostatic charging units.

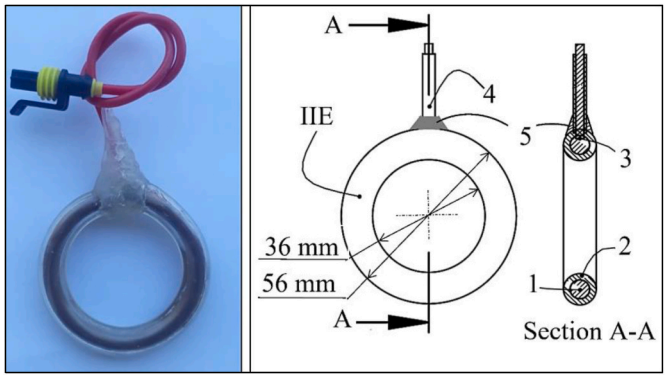


Fig. 2. Insulated induction electrode (IIE).

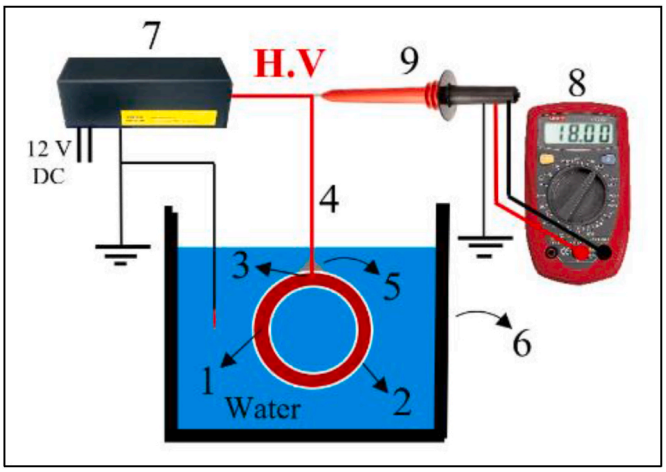


Fig. 3. Tools and equipment used to test the stability of the electrode insulation.

sprayer.

Tap water was used as a spray liquid that was forced from a tank (1) to the electrostatic charging units (2) by air pressure. A solenoid valve (3) was used to turn the spraying operation on and off. The required spraying pressure, monitored using a manometer (5) (A1001, SIMGA Instruments Co., Istanbul, Türkiye), was adjusted by the air control unit (4). A high-voltage source (6) was used to supply the required potential values with a positive signal to the insulated electrodes of the electrostatic units, which were measured with a digital voltmeter device (7) through a high-voltage probe (8). As a result, a negative electric charge was induced from the ground to the liquid jet via the earthing wire (9), which breaks up later into negatively charged droplets (10). An aluminum plate (11) with dimensions of 600 × 500 mm, which was sufficient to cover the whole spray angle of the used nozzle (80° at 500 kPa) at a distance of 250 mm from the nozzle outlet, was used to measure the electric current of each charging unit. The charged droplets striking the plate surface cause an electric current (13) that was measured by the ammeter (14) (Model Amprobe 30xr-A, Danaher Corporation, Washington, USA; Range = 0–200 μA DC, Accuracy = ± (1.5% + 1)). The air-assist velocity (15) provided by the sprayer fan was

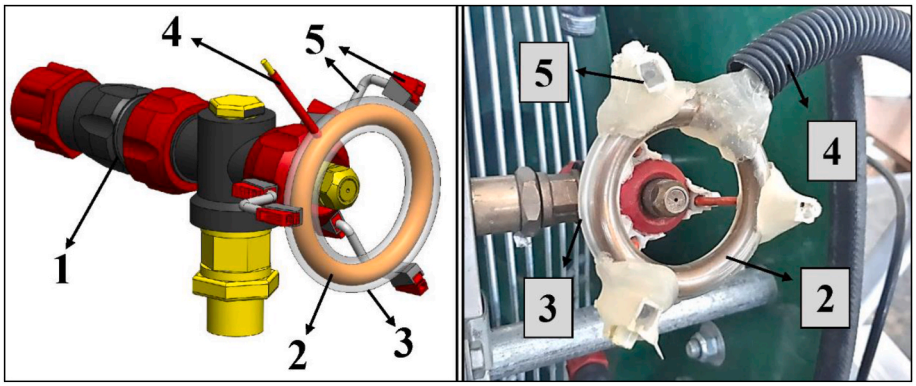


Fig. 4. Electrostatic charging unit produced for air-assisted orchard sprayer.

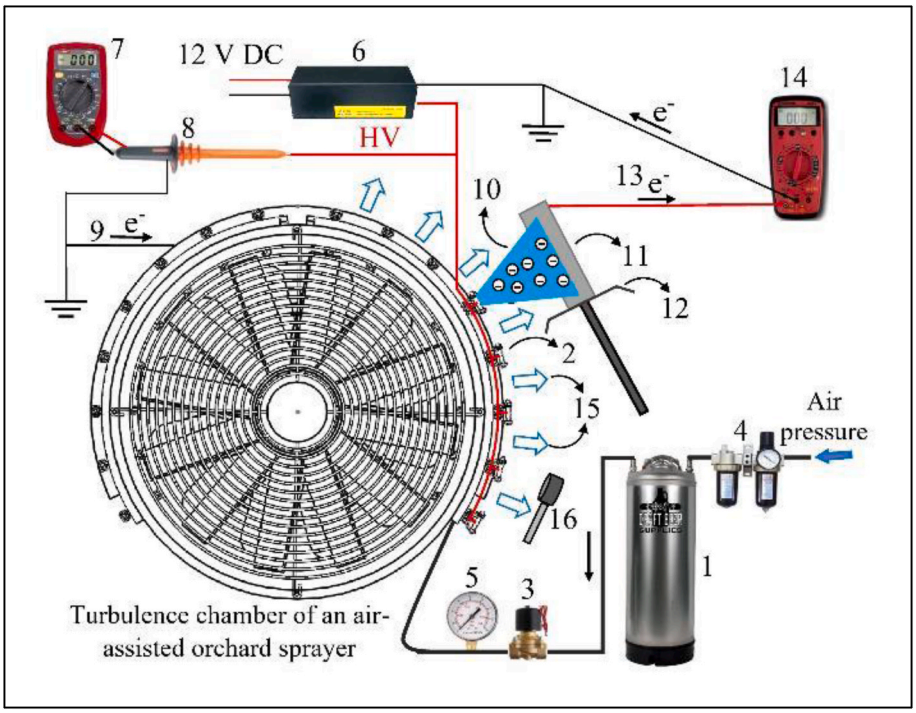


Fig. 5. Tools and equipment used to measure the electric current of charged droplets produced by electrostatic units on the sprayer.

measured with an anemometer at the air outlet of the sprayer (16) (Omega-Hhf710 - Omega Engineering Inc., Norwalk, USA).

The spray current was measured for each charging unit independently to ensure that the charged spray would not have interfered, affecting the actual results. While measuring the spray current for one of the charging units on the sprayer, the spraying operation of the other units was turned off. Moreover, the handle of the aluminum plate was made from a dielectric substance and was long enough to measure the spray current without any negative effects on the results. In addition, a dielectric protector (12) was added between the plate and the handle to prevent droplets from touching the researcher, affecting the measured results.

With a step of 2 kV, the high voltage applied to each selected charging unit was progressively increased to 16 kV at two air assist velocities of 16 and 27 m s^{-1} and a spraying pressure of 500 kPa. The average liquid flow rate of the five nozzles at the prior pressure was 386 ml min^{-1}. The charge-to-mass ratio at every measured spray current value was determined by Equation (1).

$$CMR = 60\ \frac{I_s}{Q_m} \tag{1}$$

where *CMR* (mC kg^{-1}) = charge-to-mass ratio, *Is* (μA) = electric current of the spray droplets, and Q_m (g min^{-1}) = mass flow rate of the spray liquid.

2.3. Evaluation of the deposition efficiency and ground drift potential of the electrostatic sprayer

Fig. 6 shows the electrostatic charging prototype sprayer, after mounting and testing all charging units. It included the following parts: (1) a turbulence chamber of the air-assisted conventional orchard sprayer, (2) electrostatic charging units, (3) a high voltage supply and control unit, and (4) a panel used to connect the high-voltage cables of the charging units to the main cable of the potential source (Fig. 6-A).

The performance of the prototype electrostatic-spraying machine was evaluated by comparing the difference between deposition means on the front and back surfaces of artificial and actual plant targets with and without activating the charging units, as well as the amount of droplet loss (drift) to the ground. In all deposition trials, as shown in Fig. 6-B, a tractor (5) was used to carry the prototype electrostatic sprayer and move beside the targets (6) with a forward velocity of 1.8 km h^{-1}. The spraying liquid, with the spraying pressure monitored by a manometer (7), was supplied to the sprayer by the same spraying system shown in Fig. 5 via a plastic hose (8). Cables (9) were used to ground both the targets and the sprayer. To detect spray deposition and ground drift on the targets, a spray solution containing BSF tracer (Brilliant Sulpho Flavin) was sprayed at the same amount for all spraying trials (30 g per 50-L water). The deposition experiments were performed with three repetitions for each spraying situation on and off at ambient temperature and humidity of 29 °C and 30%, respectively.

2.3.1. Artificial targets

In electrostatic spraying, the shape, orientation, and conductivity of the leaf, as well as some physiological properties of the plant, affect the charge exchange on the plant during the deposition of droplets on real plant targets (Lane and Law, 1982; Law and Lane, 1982; Maski and Durairaj, 2010; Sugimoto et al., 1999). Moreover, the air current generated by the sprayer fan causes tree branches to strongly move, potentially affecting the deposition results on the upper and lower surfaces of plant leaves. To eliminate all these variables, in addition to real plant targets, deposition trials were conducted using grounded artificial targets.

To assess artificial target deposition and spray drift on the ground, 18 aluminum plates were fixed onto three grounded metal poles and used as artificial targets for effectively evaluating the performance of the electrostatic sprayer. The surface area of each aluminum plate was 27 cm^2, and the plate edges were rounded to prevent ionization (Law and Lane, 1982). As shown in Fig. 7, each pole (1) was equipped to accommodate six plates (2) at three different heights (upper, middle, and lower). At each height, two plates (3 and 4) were positioned to quantify droplet deposition on the front and back surfaces of the target, respectively. In addition, three filter papers (30 × 20 mm) (5) were positioned beneath each pole using holders (6) and deli clips (7) to measure the spray loss to the ground. The distance between each of two poles was 1.5 m and that between the sprayer and the poles was 1 m.

In all deposition experiments on artificial targets, the average value of the charge-to-mass ratios at 14 kV applied to the induction electrodes was 0.67 mC kg^{-1} at an air velocity of 27 m s^{-1} and spraying pressure of 500 kPa (average liquid flow rate of the nozzles was 386 ml min^{-1}).

2.3.2. Real plant targets

Potted Ficus trees with dense canopies were selected to evaluate the effectiveness of the electrostatic prototype sprayer in increasing droplet deposition on real plant targets. As shown in Fig. 8, each plant was

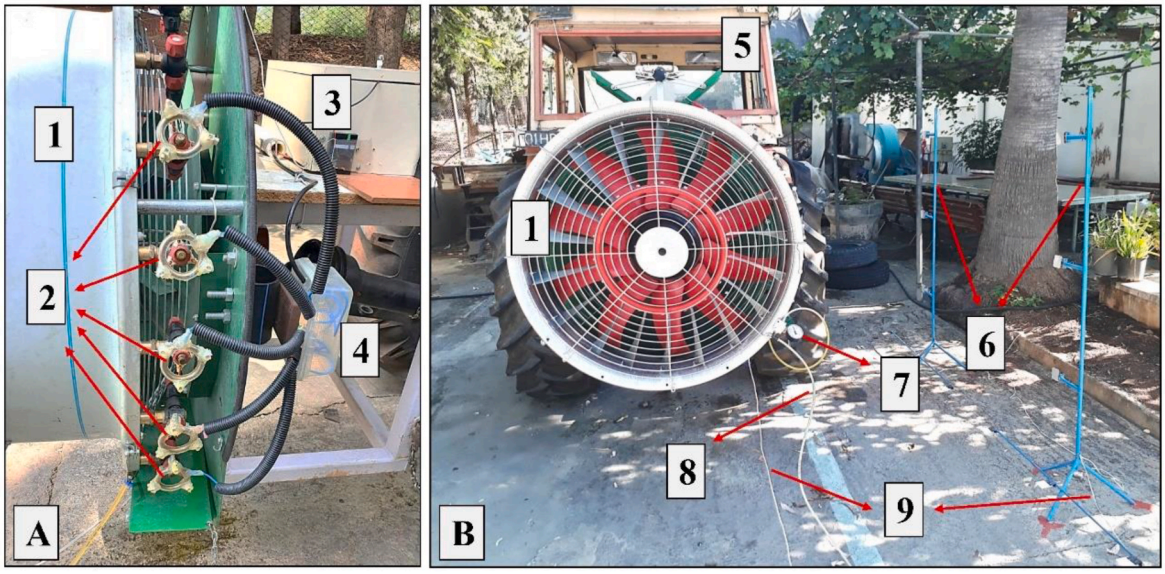


Fig. 6. Air-assisted sprayer with electrostatic charging units and the deposition trials setup.

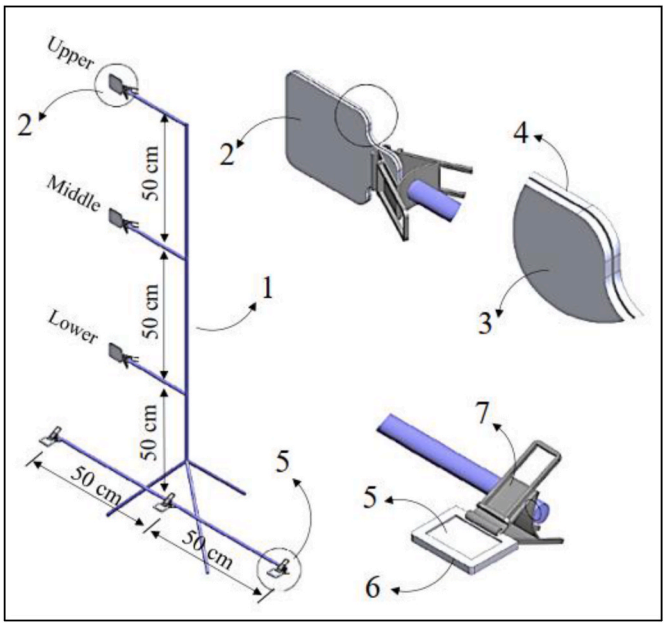


Fig. 7. Grounded metallic poles used to fix artificial targets.

divided into three heights (upper, middle, and lower), and at each selected height, sampling was conducted on two leaves in the outer part of the canopy for deposits on the leaf front surface (1). For deposition on the leaf back surface (2), sampling was performed on the underside of two other leaves at the same height but toward the inner part of the canopy. Three plants in the same row, spaced at 1.5 m intervals, were grounded by inserting 10 aluminum rods into the soil of each pot. These rods, each with a length equal to the soil height and diameter of 8 mm, were connected to an earthing wire (5). Before each spraying experiment, only the lower parts (pot soil) were irrigated to ensure good conductivity between the rods and plant roots. On the other hand, three filter papers (4), with dimensions of 30 × 20 mm, were fixed on a wood timber surface (3) below each tree to measure the amount of droplet loss to the ground surface.

An air assist velocity of only 16 m s^{-1} was used owing to the small size of the plants to minimize the impact of air current force on leaf orientations and droplet motion, which could affect the deposition results. The distance between the sprayer and the plants was also increased from 1 m to 1.5 m for the same reasons. The average charge-to-mass ratio of the electrostatic nozzles in deposition experiments on artificial targets was 0.4 mC kg^{-1} (14 kV electrode voltage) at an air assist velocity of 16 m s^{-1} and spraying pressure of 500 kPa (average liquid flow rate of the nozzles was 386 ml. min^{-1}).

2.4. Measurement of droplet deposition quantities on target surfaces

After every experiment was completed, each aluminum plate or filter paper was carefully removed and placed in a glass jar representing their region. To dissolve the BSF material from the filter papers, 50 ml of pure water was added to each jar and shaken for 30 min. The extended duration was selected because the shaking device (SL 350, Nuve Co., Ankara, Türkiye) was adjusted to operate at a low frequency to ensure the safety of the glass jars used for holding the filter paper samples. This shaking period was also previously validated to confirm that the filter paper would not disintegrate and become suspended in the solution, which could affect the results. A clean filter paper was placed in a jar with the same volume of pure water (50 ml) and subjecting it to the same 30-min shaking period. The results showed no significant difference between the intensities of the normal pure water and pure water shaken with clean filter paper.

The fluorescence intensity of BSF in each jar was measured using a fluorophotometer (RF-6000, Shimadzu Co., Kyoto, Japan). The concentration of BSF material (μg ml^{-1}) in each jar was calculated using the previously extracted standard Equation (2).

$$Y = 2131.2X + 180.052 \quad (2)$$

$$r^2 = 0.99793$$

Where Y = intensity, X = concentration values, and r^2 = coefficient of determination.

The amount of tracer material (μg) deposited per unit area of the target surface (cm^{-2}) was calculated in the same way as in previous studies (Nascimento et al., 2022; Sinha et al., 2020; Yan et al., 2024) using Equation (3).

$$f_x = \frac{m.V_L}{A} \quad (3)$$

where f_x (μg cm^{-2}) = amount of BSF material deposited on the unit sample surface, m (μg.ml^{-1}) = concentration factor, V_L (ml) = The amount of distilled water used to wash the tracer material on the filter paper and aluminum plates, *and* A (cm^2) = Area of the target surface exposed to spraying.

2.5. Statistical analysis

In this study, the collected data were used as variables to compare the average deposition amounts provided on the selected target surfaces for electrostatically charged/uncharged applications. All experimental data were analyzed using IBM SPSS 26 (Armonk, NY: IBM Corp). No data transformation was performed. T-tests were used to assess mean differences between two groups, while one-way analysis of variance (ANOVA) was employed to examine differences among three or more groups. In addition, Tukey's test was conducted to identify significant differences between the groups.

3. Results and discussion

3.1. Effect of the insulating layer on the charging performance of the induction electrode

The impact of adding an electrical insulation layer to induction electrodes on charging performance was previously evaluated in a spraying laboratory using the nozzle shown in Fig. 1-A and the Faraday cage described in a study conducted by Amaya and Bayat (2023). Table 1 presents the statistical analysis of the charge-to-mass ratios (CMR) obtained by both the uninsulated and insulated electrodes when subjected to the same increasing electrical voltage. It was noted that insulating the induction electrode resulted in a significant reduction in the charge-to-mass ratio of the spray droplets compared with that provided by the uninsulated electrode under similar spraying and charging conditions. This decline can be attributed to the distortion of the electric field between the electrode surface and liquid jet caused by the added insulating layer, which negatively impacts the charging performance. However, Table 1 shows that the uninsulated electrode, in contrast to the insulated one, fails to charge spray droplets when the voltage reaches 7 kV or higher due to electrical leakage.

The charge-to-mass ratios for voltages above 6 kV applied to the insulated electrode were statistically compared with the highest value obtained by the uninsulated electrode. The difference in the significant values of the charge-to-mass ratios obtained by both electrodes favored the uninsulated electrode until a high voltage of 9 kV was applied to the insulated electrode. This value produced a charge-to-mass ratio of 0.40 mC kg^{-1}, which was statistically equivalent to that provided by the uninsulated electrode (0.39 mC kg^{-1}) at 6 kV. After this value, the insulated electrode begins to provide charge-to-mass ratios that are

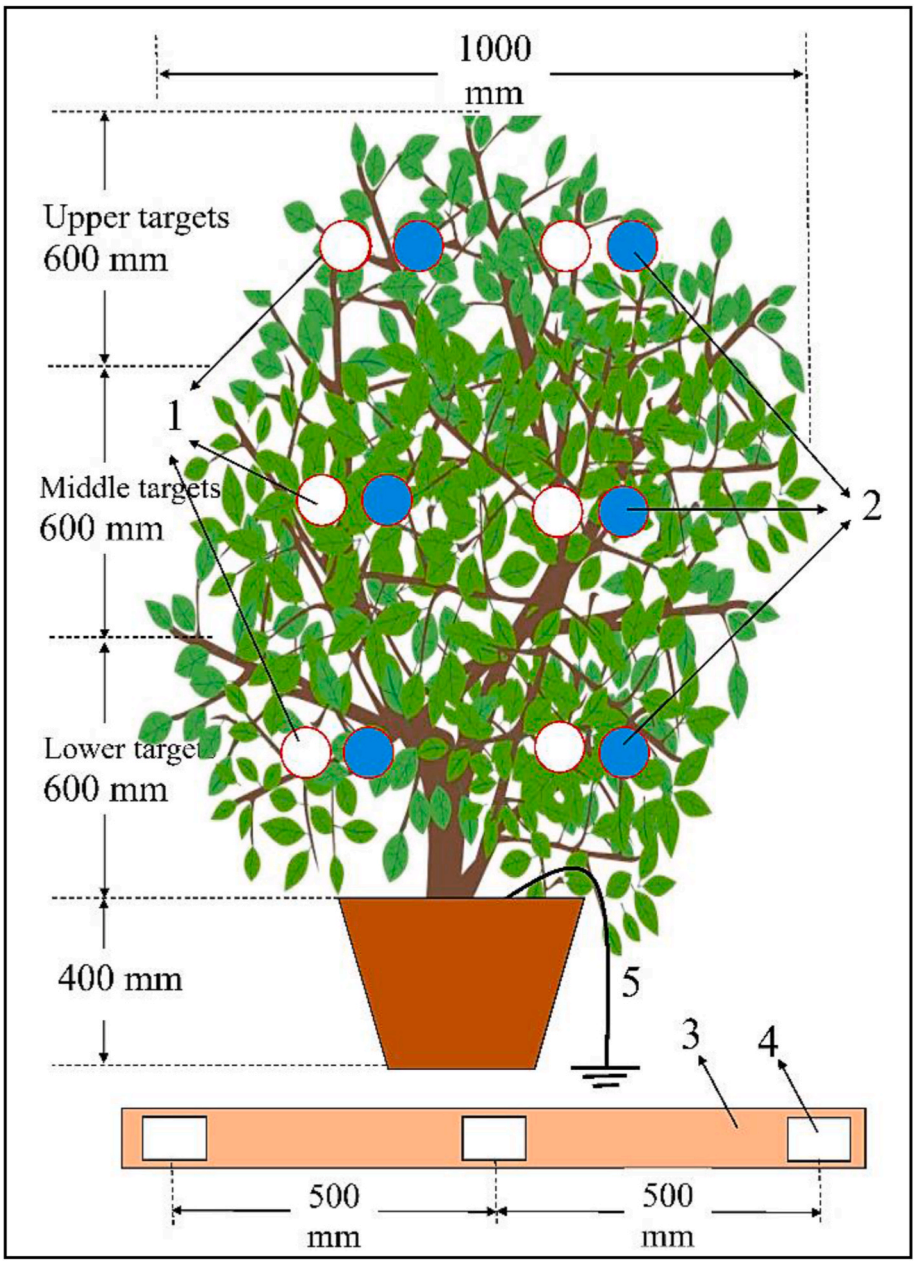


Fig. 8. Tree divided into regions to attach filter papers.

significantly higher than those obtained by the uninsulated electrode at 6 kV. The most significant value of the charge-to-mass ratio by the insulated electrode reached 0.50 mC kg^{-1} at 16 kV, with an increase of 28.37% compared with the highest value obtained by the uninsulated electrode of 0.39 mC kg^{-1} at 6 kV.

Building on the foregoing, insulated induction electrodes can provide higher charging efficiency than uninsulated ones. This presents a promising opportunity to develop low-cost and safe electrostatic charging systems, using simple high-voltage sources (Amaya, 2024), that can be seamlessly integrated with existing pesticide sprayers without requiring modifications to the original design. This approach can improve the adoption of electrostatic technology in agriculture by eliminating concerns about electrical leakage and high-voltage hazards. Moreover, improving the thickness and quality of the insulating layer can significantly improve charging performance, leading to better droplet deposition.

3.2. Charge-to-mass ratios of the insulated electrostatic units installed on the sprayer

Table 2 illustrates the average charge-to-mass ratios of the droplets produced by the electrostatic units mounted on the air-assisted orchard sprayer (Fig. 6-A), evaluated using the method shown in Fig. 5 at different electrode voltages and two air velocities.

Increasing the high voltage applied to the charging units resulted in higher average charge-to-mass ratios for both air velocities. Applying a higher voltage intensifies the electrical field between the induction electrode and the grounded liquid jet leaving the nozzle orifice. This growing electrical field induces more electric charges on the coherent liquid, thereby positively affecting the charge-to-mass ratio. At an air velocity of 16 m s^{-1}, the highest obtained value reached 0.41 mC kg^{-1} at 12 kV electrode voltage, and this value remained constant regardless of the increasing voltage level. The air velocities were probably not sufficient to remove the electrode wetting problem at high voltages, which

Table 1
Effect of electrical insulation layer on charging performance (mC kg^{-1}) of induction electrode.

Electrode Voltage (kV)	Uninsulated Electrode		Insulated Electrode		T	Change in the CMR (%)
	CMR	Std. Dev	CMR	Std. Dev		
2	0.14	0.001	0.10	0.001	−87.64***	−28.57
4	0.29	0.002	0.20	0.002	−50.91***	−31.03
6	0.39	0.002	0.29	0.002	−40.00***	−25.64
7	EL	–	0.32	0.004	−18.55***	−17.95
8	EL	–	0.36	0.004	−8.71***	−7.69
9	EL	–	0.40	0.006	2.53^{ns}	2.56
10	EL	–	0.41	0.006	4.11*	5.13
12	EL	–	0.45	0.008	10.84***	15.38
14	EL	–	0.47	0.008	15.49***	20.51
16	EL	–	0.50	0.013	14.36***	28.21

EL: Electrical leakage, significance level (ns) P-value > 0.05.* P-value <0.01.** P-value <0.05.*** P-value <0.001.

Table 2
Effect of the air velocity of the sprayer fan on the average values of the charge-to-mass ratios (CMR) obtained by the electrostatic units mounted on the sprayer (mC kg^{-1}).

Electrode Voltage (kV)	16 m s^{-1}		27 m s^{-1}		T
	CMR	Std. Dev	CMR	Std. Dev	
2.00	0.17	0.03	0.11	0.01	7.02***
4.00	0.27	0.03	0.26	0.03	1.31^{ns}
6.00	0.34	0.04	0.40	0.04	−4.09***
8.00	0.40	0.05	0.50	0.05	−4.85***
10.00	0.41	0.06	0.57	0.05	−7.31***
12.00	0.41	0.06	0.63	0.05	−10.10***
14.00	0.40	0.05	0.68	0.08	−11.69***
16.00	0.40	0.05	0.67	0.09	−10.40***

T: *t*-test, significance level: (ns) P-value > 0.05; (*) P-value <0.05; (**) P-value <0.01; (***) P-value <0.001.

led to the stopping of the increase in the charge-to-mass ratio. Especially the air velocity of 27 m s^{-1} positively affected the average charge-to-mass ratio to reach the highest value of 0.67 mC kg-1 at 16 kV, with an increasing percentage of 63%.

However, it was observed that the high-velocity airflow (27 m s^{-1}) had a detrimental impact on the charge-to-mass ratio at an electrode voltage of 2 kV, whereas it did not have any effect at 4 kV. This phenomenon can be attributed to the fact that relatively low levels of high voltage do not result in excessive wetting of the induction electrodes, which requires high air velocities. Simultaneously, high velocities widen the gap between the spray cones and the surface of the induction electrodes, reducing the electric flux density, which also negatively affects the charge-to-mass ratio. Consequently, the charge-to-mass ratio was higher at lower air velocities and electrode voltages.

These findings provide a better understanding of how the airflow velocity of the fan and the applied voltage affect the performance of electrostatic charging systems using insulated electrodes mounted on an air-assisted sprayer. Increasing the fan air velocity and applied voltage resulted in a higher CMR, and thus, stronger electrostatic attraction between charged droplets and plant foliage, enhancing spray deposition. Nevertheless, it should be considered that applying extremely high air velocities can increase the drag force of the droplets to values higher than those of electrostatic forces. Such an occurrence could yield undesired outcomes as the droplets subjected to a high drag force deviate from the intended target.

3.3. Evaluation of the electrostatic sprayer in increasing spray deposition

3.3.1. Droplet deposition on artificial and plant targets

Table 3 shows that charging spray droplets using the electrostatic units on the sprayer led to a significant increase in droplet deposition on the front and back surfaces of both artificial and plant targets compared with normal deposition conditions using the same sprayer but without activating the charging device.

When the electrostatic charging units were turned on, deposition on the front surfaces of the artificial targets increased from 1.35 μg cm^{-2} to 2.56 μg cm^{-2}, representing an 89.63% increase. On the back surfaces of the artificial targets, the activated charging units provided a deposition mean of 0.65 μg cm^{-2}, a remarkable 3250% increase compared with the normal deposition by inactive units which was only 0.02 μg cm^{-2}. Notably, the difference between normal and electrostatic deposition on the back surfaces of the artificial targets was very high. This could be attributed to the fact that the aluminum plates facing the droplet path, were strongly fixed to poles and not affected by the fan air current, which can improve deposition on back surfaces such as in the case of tree leaves. Therefore, contrary to the charged droplets that wrapped around the artificial targets and deposited on the back surfaces, there was no spray deposition on these surfaces when the charging units were off (maybe only a negligible quantity deposited on the edges).

Regarding plant targets, activating the electrostatic charging units increased deposition on the front surfaces of plant leaves from 3.16 μg cm^{-2} to 4.85 μg cm^{-2}, marking a significant 53.48% increase. Similarly, the activated charging units resulted in a deposition mean of 0.36 μg cm^{-2} on the back surfaces of plant leaves with a notable increase of 111.76% compared to the normal deposition of 0.17 μg cm^{-2}

On the other hand, it was observed that electrostatic spraying resulted in higher deposition on the back surfaces of the artificial targets relative to the amount deposited on the front surfaces. Specifically, the deposition percentage on the back surfaces relative to the front surfaces (BS/FS) increased from 1.5% under normal deposition conditions to 25% when the spray droplets were charged with static electricity. However, this percentage remained somewhat similar for both deposition types on plant leaves. In the normal spraying application, it was 5.4%, whereas it increased to 7.4% upon the activation of the electrostatic units.

In light of the aforementioned observations, electrostatic charging units with insulated electrodes can be used to increase spray deposition on the upper and lower surfaces of plant leaves. The deposition on the back surface is attributed to the wraparound phenomenon, in which charged droplets follow the trajectories of the electric field lines generated between them and the front/back surfaces of the target. These findings align with those of several previous studies on pesticide applications using electrostatic charging technology. However, the electrostatic charging nozzles used in those works had low liquid flow rates, less than 156 ml min^{-1}, and adapting them to air-assisted orchard sprayers requires changing the original design of the machine (Maski and Durairaj, 2010; Pascuzzi and Cerruto, 2015; Patel et al., 2017). In addition, some other studies installed uninsulated electrodes on air-assisted sprayers (Bayat et al., 1994; Göhlich et al., 1996; Neto et al., 2015). However, these electrostatic spraying machines required high air velocities of up to 78 m s^{-1} to prevent electrical leakage. Such high velocities may counteract the desired electrostatic forces, thereby reducing the deposition amount.

The advantages of the innovative charging units in this study encourage farmers to use electrostatic spray technology for pesticide applications in orchards using existing air-assisted sprayers, without the need to buy expensive new equipment. With the aid of the adjustable connection tools (5) shown in Fig. 4, these units can be readily attached to or detached from the nozzles mounted on the sprayer as required. One of the key features of these units is their ability to safely facilitate electrostatic pesticide applications without the concerns associated with high voltages. Moreover, thanks to the insulation layer that prevents

Table 3
Mean deposition (±SD) on the front surfaces (FS) and back surfaces (BS) of all artificial and plant targets.

Charging units	Deposition on artificial targets					Deposition on plant targets				
	FS (μg cm^{-2})	CV (%)	BS (μg cm^{-2})	CV (%)	BS/FS (%)	FS (μg cm^{-2})	CV (%)	BS (μg cm^{-2})	CV (%)	BS/FS (%)
OFF	1.35 ± 0.23	17	0.02 ± 0.01	50	1.5	3.16 ± 1.65	52	0.17 ± 0.06	35	5.4
ON	2.56 ± 0.52	20	0.65 ± 0.22	34	25	4.85 ± 2.41	50	0.36 ± 0.15	42	7.4
df	52	–	52	–	–	52		52	–	–
T	−11.0***	–	−14.9***	–	–	−3.0***		−5.8***	–	–
CP	+89.63 %	–	+3250 %	–	–	+53.48 %		+111.76 %	–	–

CV: coefficient of variation, df: degree of freedom, T: *t*-test, CP: change percentage in the deposition means, significance level: (ns) P-value greater than 0.05; (*) P-value <0.05; (**) P-value <0.01; *** P-Value <0.001.

electrical leakage, the air velocity of the sprayer fan can be adjusted with the values that provide the most spray deposition without facing any electrical leakage problems.

3.3.2. Effect of target height on average deposition

As shown in Table 4, the statistical analysis revealed that the activation of the electrostatic charging units led to a significant increase in the deposition amounts on the front surfaces of all artificial targets positioned at different heights. The deposition amounts on the front surfaces of the upper, middle, and lower targets increased from 1.25, 1.53, and 1.28 μg cm^{-2} to 2.18, 2.96, and 2.54 μg cm^{-2}, respectively, representing increases of 74.4%, 93.5%, and 98.4%, respectively. Similarly, Table 5 shows that electrostatic charging significantly increased the deposition amounts on the back surfaces of the upper, middle, and lower artificial targets from normal deposition values 0.018, 0.022, and 0.018 μg cm^{-2} to 0.654, 0.760, and 0.543 μg cm^{-2}, respectively, representing increases of 3600%, 3454%, and 3016%, respectively.

Regarding deposition on plant targets at varying heights, it is noteworthy that the statistical analysis revealed a significant increase in the deposition amounts on the front surfaces for only the lower targets upon activation of the electrostatic charging units (Table 6), with an increase of 93.37%. Conversely, the increases in deposition on the front surfaces of the upper and middle targets were less substantial, with increases of 38.72% and 31.14%, respectively, which were not statistically significant. On the other hand, activating the charging units led to a significant increase in deposition on the back surfaces of all plant targets positioned at three different heights, as detailed in Table 7. The deposition amounts on the back surfaces of the upper, middle, and lower plant targets increased from 0.10, 0.20, and 0.23 μg cm^{-2} to 0.19, 0.41, and 0.47 μg cm^{-2}, respectively, representing increases of 90.00%, 100.05%, and 100.04%, respectively.

3.3.3. Effect of electrostatic charging on the deposition distribution across the heights of the targets

Understanding how electrostatic charging of droplets affects deposition distribution across targets at different heights is crucial for improving pesticide application efficiency using electrostatic spraying technology on trees with complex geometric shapes.

Table 4
Mean deposition (μg cm^{-2}) ± SD on the front surfaces of artificial targets at different three heights.

Charging units	Target position			df	F
	Upper	Middle	Lower		
OFF	1.25b ± 0.14	1.53a ±0.27	1.28b ± 0.18	2	4.91*
ON	2.18b ± 0.41	2.96a ±0.34	2.54 ab ± 0.49	2	7.74**
df	16	16	16	–	–
T	−6.4***	−9.8***	−7.2***	–	–
CP	+74.4 %	+93.5 %	+98.4 %	–	–

T: *t*-test, df: degree of freedom, CP: change percentage in the deposition means, significance level: (ns) P-value greater than 0.05.* P-value <0.05.** P-value <0.01.*** P-value <0.001.

Table 5
Mean deposition (μg cm^{-2}) ± SD on the back surfaces of artificial targets at different three heights.

Charging units	Target position			df	F
	Upper	Middle	Lower		
OFF	0.018 ± 0.008	0.022 ± 0.010	0.018 ± 0.008	2	0.76^{ns}
ON	0.654 ± 0.144	0.760 ± 0.244	0.543 ± 0.227	2	2.40^{ns}
df	16	16	16	–	–
T	−13.2***	−9.0***	−6.9***	–	–
CP	+3600%	+3454%	+3016%	–	–

T: *t*-test, df: degree of freedom, CP: change percentage in the deposition means, significance level: (ns) P-value greater than 0.05; (*) P-value <0.05; (**) P-value <0.01; *** P-value <0.001.

Table 6
Mean deposition (μg cm^{-2}) ± SD on the front surfaces of plant targets at different three heights.

Charging units	Target position			df	F
	Upper	Middle	Lower		
OFF	2.97 ± 1.46	3.50 ± 1.80	3.02 ± 1.83	2	0.26^{ns}
ON	4.12 ± 1.63	4.59 ± 1.61	5.84 ± 3.44	2	1.20^{ns}
df	16	16	16	–	–
T	−1.6ns	−1.3ns	−2.2*	–	–
CP	+38.72 %	+31.14 %	+93.37 %	–	–

T: *t*-test, df: degree of freedom, CP: change percentage in the deposition means, significance level: (ns) P-value greater than 0.05.(**) P-value <0.01; (***) P-value <0.001; *** P-value <0.05.

Table 7
Mean deposition (μg cm^{-2}) ± SD on the back surfaces of plant targets at different three heights.

Charging units	Target position			df	F
	Upper	Middle	Lower		
OFF	0.10b ± 0.02	0.20a ±0.04	0.23a ±0.02	2	50.1***
ON	0.19b ± 0.01	0.41a ±0.14	0.47a ±0.09	2	21.0***
df	16	16	16	–	–
T	−15.0***	−4.4***	−8.1***	–	–
CP	+90.00 %	+100.05 %	+100.04 %	–	–

T: *t*-test, df: degree of freedom, CP: change percentage in the deposition means, significance level: (ns) P-value greater than 0.05; (*) P-value <0.05; (**) P-value <0.01; *** P-value <0.001.

As shown in Table 4, the deposition quantities on the front surfaces were significantly greater at the middle artificial targets in both spraying situations than those at the upper and lower heights, which had similar deposition distributions. Conversely, deposition quantities on the back surfaces did not show significant differences across all heights, regardless of the spraying application method (Table 5). For plant targets, similarly, the deposition quantities on the front surfaces of the leaves

were not significantly different between all heights, independent of the spraying application method (Table 6). However, in terms of deposition on the back surfaces, in both spraying cases with and without electrostatic charging, the plant targets at middle and lower heights obtained equivalent quantities of spray droplets, which were larger than those obtained at the upper targets (Table 7).

Consequently, the electrostatic charging of liquid droplets did not significantly affect the deposition distribution across the target heights. Therefore, other factors such as nozzle type, airflow dynamics, environmental conditions, or plant target geometry may play a more significant role than electrostatic forces in determining the deposition patterns of sprayed droplets across varying target heights.

3.3.4. Losses to the ground

In pesticide applications, a large portion of spray droplets can be lost or diverted away from the intended target, potentially leading to off-target deposits or soil loss.

In deposition experiments on the artificial targets, Table 8 shows that activating the electrostatic charging units led to a significant increase in droplet loss to the ground from 0.05–0.2 μg cm^{-2}, representing an increase of 400% compared with the average loss quantities of uncharged droplets. This unexpected behavior may be attributed to the influence of the grounded metal pipe adjacent to the filter papers, as depicted in Fig. 7. The filter paper likely received more droplets because of the electric attraction between the charged droplets and the nearby pipe.

In contrast, the filter papers used to measure the droplet loss quantities to the ground in deposition trials on real plant targets were positioned away from any nearby grounded objects (Fig. 8). No significant difference in droplet loss to the ground was noted between charged and uncharged droplets during these trials. When the electrostatic charging units were activated, there was only a slight increase (without statistical significance) in droplet loss to the ground, from 0.36 to 0.39 μg cm^{-2}, with an increase of +8.33%. These results were contrary to the findings of studies conducted by (De Assunção et al., 2020; Neto et al., 2015) that showed the ability of electrostatic sprayers to reduce spray losses to the ground. However, the air current in this study was likely responsible for the non-changing droplet loss quantities to the ground when activating the charging units. Perhaps the spray droplets were carried far from the ground targets during spraying, whether or not electrostatic charging was activated.

Notably, the consistent ground loss amounts during the plant target trials support the hypothesis regarding the impact of the metal pipe on ground loss during the experiments on artificial targets.

3.3.5. Uniformity of spray distribution on the front and back surfaces of the targets

The coefficient of variation (CV%) for mean deposition in each treatment was calculated in the same way as in previous studies (Musiu et al., 2019; Sánchez-Hermosilla et al., 2012). The aim was to assess the impact of activating the electrostatic units on the distribution uniformity of deposition on the front and back surfaces of the artificial and plant targets, as well as on the targets positioned to measure spray losses to the ground.

During the deposition trials on the artificial targets, Table 3 shows that activating the electrostatic charging units resulted in a minor negative change in distribution of droplets on the front surfaces, from 17% to 20%. The electrostatic spraying application, on the other hand, enhanced the distribution uniformity on the back surfaces and on the targets positioned to measure droplet loss to the ground from the values of 50% and 60% achieved by uncharged droplets, to 34% and 35%, respectively.

Regarding deposition distribution on the plant targets, Table 3 indicates that activating the electrostatic charging units affected neither the droplet distribution on the front surfaces nor on the targets designated to assess droplet loss to the ground. There was a slight improvement in the distribution uniformity, from 52% to 50% for the front surfaces and from 33% to 28% for the ground targets. In contrast, the homogeneity of spray droplets on the back surfaces of the plant targets got worse, changing from 35% to 42% when the electrostatic units were activated to charge the spray droplets.

The conclusions regarding distribution uniformity on the plant targets in this study differ from the findings of previous similar studies, which declared that activating the electrostatic sprayer improves uniformity on plant targets (Patel et al., 2017; Salcedo et al., 2020). At the same time, they align with the findings of a study by (Salcedo et al., 2023), which showed that activated charging devices did not enhance the distribution of plant droplets.

Table 8
Loss quantities to the ground GL (μg cm^{-2}) ± SD.

Charging units	Artificial target trials		Plant target trials	
	GL (μg cm^{-2})	CV (%)	GL (μg cm^{-2})	CV (%)
OFF	0.05 ± 0.03	60	0.36 ± 0.12	33
ON	0.20 ± 0.07	35	0.39 ± 0.11	28
df	52		52	
T	−10.0***		-1.0^{ns}	
CP	+400 %		+8.33 %	

T: *t*-test, CV: coefficient of variation, df: degree of freedom, CP: change percentage in the deposition means, Significance level: (ns) P-Value greater than 0.05; (*) P-Value <0.05; (**) P-value <0.01; *** P-Value < 0.001.

4. Conclusion

This study presents a cost-effective electrostatic charging system designed for integration into conventional air-assisted orchard sprayers without alterations to the original machine design. The novel charging device, which is characterized by its ability to charge spray droplets using induction electrodes isolated from the external environment, offers a promising avenue for enhancing the adoption of electrostatic technology in agriculture. This is achieved by addressing safety concerns related to high-voltage hazards. Furthermore, the inclusion of an insulation layer in the system permits the adjustment of the sprayer fan's air velocity to achieve optimal spray deposition without the risk of electrical leakage.

The electrostatic system demonstrated a notable average charge-to-mass ratio of 0.67 mC kg^{-1} at an electrode voltage of 14 kV and an air-assisted velocity of 27 m s^{-1}. Activation of the charging system resulted in a significant increase in droplet deposition on artificial targets, with a 0.90-fold increase on the front surfaces and a 32.5-fold increase on the back surfaces compared with standard uncharged spraying conditions. Similarly, for plant leaves, the activated electrostatic spraying system yielded a 0.54-fold increase on the front surfaces and a 1.12-fold increase on the back surfaces compared with uncharged droplet deposition.

Future research will focus on optimizing the thickness and quality of the insulating layer to enhance the charging performance of the system, thereby positively impacting the deposition of droplets. In addition, further studies are needed to better understand the electrostatic charging impacts on the uniformity of spray distribution across different target surfaces and heights.

Funding sources

This project was funded by Çukurova University Scientific Research Projects Unit - Türkiye. Project number: FDK-2019-12208

CRediT authorship contribution statement

Kemal Amaya: Writing – review & editing, Writing – original draft, Software, Investigation, Formal analysis, Data curation. **Ali Bayat:** Writing – review & editing, Writing – original draft, Supervision, Project

administration, Methodology, Investigation, Funding acquisition, Data curation.

Declaration of generative AI and AI-assisted technologies in the writing process

Due to the authors being non-native English speakers, they utilized Quillbot, OpenPaperpal, Copilot, and ChatGPT 3.5 services to improve readability and language. After using these services, the authors reviewed and edited the content as needed and take full responsibility for the content of the publication.

Declaration of competing interest

The authors declare that they have no known competing financial interests or personal relationships that could have appeared to influence the work reported in this paper.

Data availability

Data will be made available on request.

Abbreviations

CMR	Charge-to-Mass Ratio
mC	Milli Coulomb
μA	Micro Ampere

References

Amaya, K., 2024. Low-cost high voltage generator for electrostatic charging of pesticide droplets, and laboratory uses. Gazi J. Eng. Sci. 9, 422–434. https://doi.org/10.30855/gmbd.07050776.

Amaya, K., Bayat, A., 2023. Determining effects of induction electrode geometry on charging efficiency of droplets in pesticide electrostatic spraying applications. Smart Agric. Technol. 4, 1–7. https://doi.org/10.1016/j.atech.2023.100190.

Bayat, A., Zeren, Y., Ulusoy, M.R., 1994. Spray deposition with conventional and electrostatically-charged spraying in citrus trees. Ama, Agric. Mech. Asia, Afr. Lat. Am. 25, 35–39.

De Assunção, H.H.T., Da Cunha, J.P.A.R., Silva, S.M., Alves, G.S., Lemes, E.M., 2020. Spray deposition on maize using an electrostatic sprayer. Eng. Agric. 40, 503–510. https://doi.org/10.1590/1809-4430-Eng.Agric.v40n4p503-510/2020.

Frost, A.R., Law, S.E., 1981. Extended flow characteristics of the embedded-electrode spray-charging nozzle. J. Agric. Eng. Res. 26, 79–86. https://doi.org/10.1016/0021-8634(81)90128-1.

Gan-Mor, S., Ronen, B., Ohaliav, K., 2014. The effect of air velocity and proximity on the charging of sprays from conventional hydraulic nozzles. Biosyst. Eng. 121, 200–208. https://doi.org/10.1016/j.biosystemseng.2014.03.004.

Garcera, C., Moltó, E., Chueca, P., 2017. Spray pesticide applications in Mediterranean citrus orchards: canopy deposition and off-target losses. Sci. Total Environ. 599–600, 1344–1362. https://doi.org/10.1016/j.scitotenv.2017.05.029.

Göhlich, H., Ganzelmeier, H., Bäcker, G., 1996. Air-assisted sprayers for application in vine, orchard and similar crops. EPPO Bull. 26, 53–58. https://doi.org/10.1111/j.1365-2338.1996.tb01528.x.

Herzog, G.A., Lambert, W.R., Law, S.E., Seigler, W.E., Giles, D.K., 1983. Evaluation of an electrostatic spray application system for control of insect pests in cotton. J. Econ. Entomol. 76, 637–640. https://doi.org/10.1093/jee/76.3.637.

Lane, M.D., Law, S.E., 1982. Transient charge transfer in living plants undergoing electrostatic spraying. Trans. ASAE (Am. Soc. Agric. Eng.) 25, 1148–1153. https://doi.org/10.13031/2013.33687.

Law, S.E., 1978. Embedded-electrode electrostatic-induction spray-charging nozzle: theoretical and engineering design. Trans Am Soc Agric Eng (Gen Ed) 21, 1096–1104. https://doi.org/10.13031/2013.35448.

Law, S.E., Lane, M.D., 1982. Electrostatic deposition of pesticide sprays onto ionizing targets: charge- and mass-transfer analysis. IEEE Trans. Ind. Appl. IA-18, 673–679. https://doi.org/10.1109/TIA.1982.4504125.

Martin, D.E., Latheef, M.A., Duke, S.E., 2022. Gap optimization of electrostatic aerial spray nozzles for low-speed aircraft. J. Electrost. 117, 103714 https://doi.org/10.1016/j.elstat.2022.103714.

Maski, D., Durairaj, D., 2010. Effects of charging voltage, application speed, target height, and orientation upon charged spray deposition on leaf abaxial and adaxial surfaces. Crop Protect. 29, 134–141. https://doi.org/10.1016/j.cropro.2009.10.006.

Miranda-Fuentes, A., Rodríguez-Lizana, A., Gil, E., Agüera-Vega, J., Gil-Ribes, J.A., 2015. Influence of liquid-volume and airflow rates on spray application quality and homogeneity in super-intensive olive tree canopies. Sci. Total Environ. 537, 250–259. https://doi.org/10.1016/j.scitotenv.2015.08.012.

Musiu, E.M., Qi, L., Wu, Y., 2019. Spray deposition and distribution on the targets and losses to the ground as affected by application volume rate, airflow rate and target position. Crop Protect. 116, 170–180. https://doi.org/10.1016/j.cropro.2018.10.019.

Nascimento, R.S.M., Ferreira, L.R., Zambolim, L., Parreira, D.F., Oliveira, P.L.d.S., Moraes, R.G.S., 2022. Influence of spraying tips on the efficiency of chemical control of soybean rust. Crop Protect. 160, 106031 https://doi.org/10.1016/j.cropro.2022.106031.

Neto, J.G., da Cunha, J.P.A.R., Almeida, V.V., Alves, G.S., 2015. Spray deposition on coffee leaves from airblast sprayers with and without electrostatic charge. Biosci. J. 31, 1296–1303. https://doi.org/10.14393/BJ-v31n5a2015-26876.

Pascuzzi, S., Cerruto, E., 2015. Spray deposition in “tendone” vineyards when using a pneumatic electrostatic sprayer. Crop Protect. 68, 1–11. https://doi.org/10.1016/j.cropro.2014.11.006.

Pascuzzi, S., Cerruto, E., Manetto, G., 2017. Foliar spray deposition in a “tendone” vineyard as affected by airflow rate, volume rate and vegetative development. Crop Protect. 91, 34–48. https://doi.org/10.1016/j.cropro.2016.09.009.

Patel, M.K., Kundu, M., Sahoo, H.K., Nayak, M.K., 2016. Enhanced performance of an air-assisted electrostatic nozzle: role of electrode material and its dimensional considerations in spray charging. Eng. Agric. Environ. Food 9, 332–338. https://doi.org/10.1016/j.eaef.2016.05.002.

Patel, M.K., Praveen, B., Sahoo, H.K., Patel, B., Kumar, A., Singh, M., Nayak, M.K., Rajan, P., 2017. An advance air-induced air-assisted electrostatic nozzle with enhanced performance. Comput. Electron. Agric. 135, 280–288. https://doi.org/10.1016/j.compag.2017.02.010.

Pelegrini, G., Souza, A.M., Ferreira, P.H.U., Monteiro, G.G., Ferreira, M.C., 2022. Air-assisted spraying and electrically charged droplets for Bemisia tabaci control in soybeans. Pest Manag. Sci. 78, 4618–4627. https://doi.org/10.1002/ps.7082.

Salcedo, R., Llop, J., Campos, J., Costas, M., Gallart, M., Ortega, P., Gil, E., 2020. Evaluation of leaf deposit quality between electrostatic and conventional multi-row sprayers in a trellised vineyard. Crop Protect. 127, 104964 https://doi.org/10.1016/j.cropro.2019.104964.

Salcedo, R., Sánchez, E., Zhu, H., Fàbregas, X., García-Ruiz, F., Gil, E., 2023. Evaluation of an electrostatic spray charge system implemented in three conventional orchard sprayers used on a commercial apple trees plantation. Crop Protect. 167, 106212 https://doi.org/10.1016/j.cropro.2023.106212.

Sánchez-Hermosilla, J., Rincón, V.J., Páez, F., Fernández, M., 2012. Comparative spray deposits by manually pulled trolley sprayer and a spray gun in greenhouse tomato crops. Crop Protect. 31, 119–124. https://doi.org/10.1016/j.cropro.2011.10.007.

Sinha, R., Ranjan, R., Khot, L.R., Hoheisel, G.A., Grieshop, M.J., 2020. Comparison of within canopy deposition for a solid set canopy delivery system (SSCDS) and an axial–fan airblast sprayer in a vineyard. Crop Protect. 132, 105124 https://doi.org/10.1016/j.cropro.2020.105124.

Sugimoto, T., Tanaka, S., Higashiyama, Y., Asano, K., 1999. Formation of a charged droplets cloud and corona discharge between the cloud and a grounded electrode. IEEE Trans. Ind. Appl. 35, 225–230. https://doi.org/10.1109/28.740870.

Yan, C., Tan, H., Niu, C., Shen, C., Xu, L., 2024. Spray deposition in an artificial grapevine canopy as affected by spray angle regulation systems of radial airflow air-assisted sprayers. Crop Protect. 178, 106588 https://doi.org/10.1016/j.cropro.2024.106588.